

Capabilities and limits for ADVP measurements of breaking waves and bores

Giuseppe Roberto Tomasicchio *

Engineering Department, University of Lecce, Via per Monteroni, 73100 Lecce, Italy

Received 30 December 2003; received in revised form 30 December 2004; accepted 19 September 2005

Available online 28 November 2005

Abstract

This paper presents experience from the use of an Acoustic Doppler Velocity Profiler in the surf zone over a large-scale experimental barred beach. In the first part of the paper, attention is focused on the description of a proper ADVP set-up and on the determination of relationships for the horizontal and vertical velocity components valid for the oscillatory flow case. In the second part, horizontal velocity component data from the ADVP are compared to the pre-processed measurements from two other velocity measuring devices for breaking waves, as well as near the end of the surf zone. As expected, in the outer region of the surf zone velocity measurements appear influenced by air entrainment. In the bore-like region where the effects of wave breaking are less intense and where the wave is reforming, the horizontal velocity is in reasonable agreement with the rest of the measurements. Although the ADVP appears much noisier than other instruments, the role of bubbles in outer zone is prevalent in its measuring error and gives a large underestimation. Furthermore, for the adopted experimental conditions, the analysis shows that the use in the bore-like region of relationships for the horizontal velocity component that are valid for a uniform flow generates a negligible error.

© 2005 Elsevier B.V. All rights reserved.

Keywords: Acoustic Doppler Velocity Profiler; Oscillatory flow; Wave breaking; Bore-like breaker; Bubble; Undertow; Velocity measurement

1. Introduction

The prediction of the wave-induced sediment transport at beaches needs the accurate representation of the wave kinematics at the surf zone. With reference to the field and laboratory beaches, careful measurements are generally conducted by means of Electro-Magnetic Currentmeters, Acoustic Doppler Velocimeters, Laser Doppler Velocimeters, Particle Image Velocimetry and also Hot Wire and Hot Film Anemometers. Researchers select the most appropriate instrument to use on the basis of the desired sampling frequency, length scale and type of phenomena to be observed. In particular, in the last two decades, advances in measuring techniques have made possible the accurate measurement of the internal velocity field within the surf zone and the related process of energy transfer due to turbulence [e.g. Stive, 1980; Nadaoka and Kondoh, 1982; Okayasu, 1989; Ting and Kirby, 1994; Cox et al., 1994, 1995; Doering and Donelan, 1997; Cox and Kobayashi, 2000].

More recently, experiments in hydraulics have used a new tool represented by the Acoustic Doppler Velocity Profiler (ADVP) that was initially proposed for medical applications. ADVP is a non-intrusive measuring device, acknowledged for several advantages with respect to other fluid measurement instruments. It gives highly detailed spatial–temporal information on velocity independently of seeding concentration and fluid opacity (Eckert and Gerbeth, 2002). The capability that makes the ADVP most attractive to coastal researchers is the near-simultaneous acquisition of the flow velocity projected along the sensor axis avoiding uncertainty from the repetition of the test.

Experimental studies providing information on air bubble influence on velocity measurements in fluid flows using Doppler based ultrasound techniques are scarce (Nielsen et al., 1999; Longo, submitted for publication). In particular, Longo (submitted for publication) generated two-phase flows (air or hydrogen bubbles and water) in a controllable manner and measured velocity with ADVP and ADV in order to quantify the influence of bubbles on measurements; the main conclusions are that measurements of velocity using ultrasound Doppler based velocimeters in a two-phase flow field give substantially the velocity of the bubbles, and that for a bubble

* Fax: +39 080 5213516.

E-mail address: tomicchio@dds.unical.it.

volume fraction less than 0.1 the ultrasound celerity is unaffected by bubble presence.

Optical and acoustic instruments have been used to measure the bubble size distributions inside breaking waves in the laboratory and in the open ocean (Leighton et al., 1996; Deane, 1997; Deane and Stokes, 1999; Farmer et al., 2001) with the scope to investigate on the bubble’s evolution in density, radius and spatial distribution. It has been found (Deane and Stokes, 2002) that for bubbles larger than about 1 mm, turbulent fragmentation determines bubble size distribution, resulting in a bubble density proportional to the bubble radius to the power of $-1/3$. Smaller bubbles are induced by jet and drop impact on the wave face, with a $-3/2$ power-law scaling. The length scale where turbulent fragmentation ceases, also known as Hinze scale, separates these two processes.

An ADVP has been used to measure the near-instantaneous horizontal velocity profiles induced by a breaking wave along the entire depth on a laboratory quasi-field barred beach. A similar investigation was conducted by Longo et al. (2001) who considered a small-scale experiment with sinusoidal waves propagating over a monotonic sloped beach. They

performed velocity measurements with an ADVP and an LDV in the outer and inner surf zone; data comparison was not possible because the ADVP signal was useless during the Laser series.

The present study intends to investigate on the capabilities and limits of an ADVP for measuring velocities induced by spilling and plunging breaking waves in the outer region and by bore-like breakers in the inner region. Horizontal velocity components from the ADVP are compared with the pre-processed measurements from the Acoustic Doppler Velocimeters (ADVLab) and from the Electro-Magnetic Current-meters (ECM). The determination of theoretical expressions for the horizontal and vertical velocity components induced by an oscillatory flow allows discussion of the uncertainties from the use of the relationships with validity restricted to the uniform flow case.

2. Experimental set-up and procedure

A large-scale laboratory experiment on wave hydrodynamics over a fixed-bed barred beach was performed at the wave

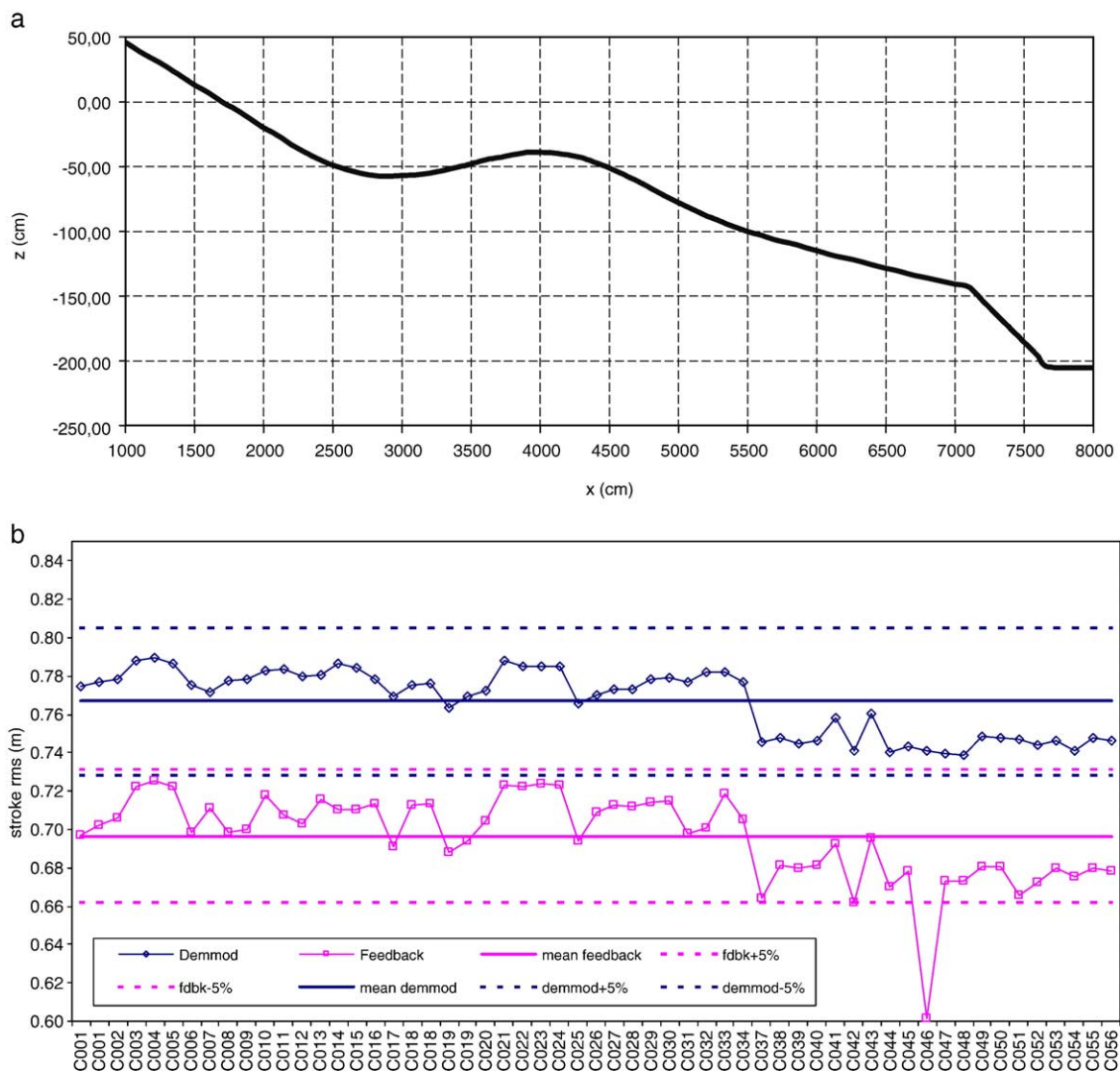


Fig. 1. (a) The geometry of the adopted beach profile. (b) Repetition number vs. stroke root-mean-square: wave condition C.

flume of the Polytechnic University of Catalonia (Barcelona), which is 100 m long, 3 m wide and 5 m deep. The adopted beach profile geometry is shown in Fig. 1a with the vertical coordinate z positive upward and $z=0$ at the still water level, waves propagating from right to left, and the wavemaker positioned at $x=8600$ cm, with x indicating the horizontal position along the flume. The water depth at the wave generator was 205 cm. The rigid bottom profile was designed to match an equilibrium bar. This was accomplished by scaling-down prototype profiles at Duck (North Carolina, USA), taking into account the SUPERTANK (Kraus and Smith, 1994) and DELTA-flume (Sanchez-Arcilla et al., 1995) movable-bed experiments. The final “equilibrium-bar” shape for the target wave conditions was tuned with the assistance of a numerical Boussinesq-type wave model (Kennedy et al., 1999) with an undertow and sediment transport formulation allowing the prediction of sediment fluxes due to the combined wave and current action and information on tendencies for onshore/offshore sediment transport (Sancho, 1999).

Three regular and one irregular wave conditions were produced by a piston type wavemaker equipped with an active reflection absorption system. Table 1 summarises the characteristics of the wave conditions, where H and H_{rms} are the regular and root-mean-square wave height, respectively, in front of the wavemaker; T_p is the peak wave period; L is the computed wavelength at the wavemaker (using linear wave theory); x_b , H_b and d_b are the approximate breaking location, breaking height and depth, respectively. The Ursell number has been defined as $U_r \equiv \frac{L^2 H}{h^3} = \frac{16}{3} K^2 \kappa^2$ (Dean and Dalrymple, 1984; USACE, 1998) where κ is the Jacobian elliptic function modulus and $K(\kappa)$ is the complete elliptic integral of the second kind (Sarpkaya and Isaacson, 1981). Free-surface elevation was registered at 49 different transects by a combination of eight conductivity-type wave gauges with 8-Hz sampling frequency. Three surface elevation sensors remained at fixed positions the whole experiment, in front of the wave paddle, for repeatability and quality control of the tests. The adopted wave conditions were run sequentially for each test repetition. In order to achieve stationarity of each sea-state, the data acquisition was started 360 s after the start of the wavemaker. Regarding quality control, and since the experiments reflected over 56 repetitions of the same wave condition, for four distinct situations, test repeatability was assessed (Sancho et al., 2001; Tomasicchio et al., 2001). Four data acquisition channels were associated, for all tests, to the wave generation/absorbing system. Namely, the four channels correspond to the following signals: (i) “DEMAND”—the original, requested, (demanded) wave generator x -position (stroke); (ii) “DEMOD”—the modified demanded signal,

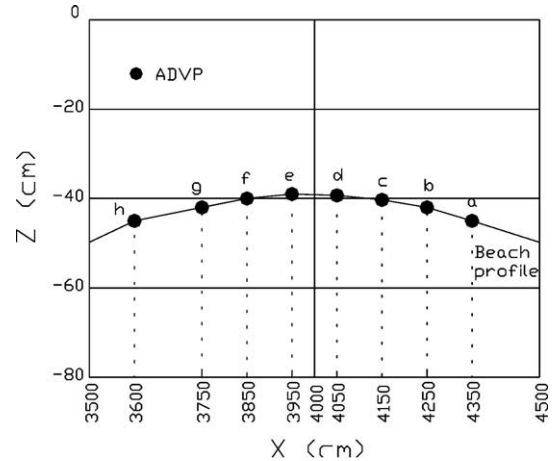


Fig. 2. Cross section of the bar and location of the measurement transects.

based on feedback information of the reflected waves; (iii) “FEEDBACK”—the actual (real) paddle x -position; (iv) “ERROR”—a measure of the difference between the “demmod” and “feedback” signals.

The wavemaker paddle position allows controlling the test repeatability. With regard to the paddle stroke position, Fig. 1b shows, for all repetitions of wave condition C, the root-mean-square stroke, based on the “demmod” and “feedback” signals of the paddle control. The upper lines refer to the “demmod” signal, whereas the lower lines represent the “feedback”. The solid-thick lines represent the average of the measured values of all repetitions and the dashed lines represent the average plus or minus 5%. Therefore, for each signal type, the band within the $\pm 5\%$ of the average values is portrayed. All runs whose signals are enclosed within those limits are considered valid and, therefore, form the basis to characterise each single wave condition experiment, with variables measured at multiple points, non-simultaneously, and representative of the same event. Based on the above analysis, 5 tests for wave condition A, 1 for wave B and 1 for wave C have been discarded from the experimental data base.

Velocity measurements were conducted with three different types of velocimeters at eight different transects along the bar (Fig. 2). Seven spherical S-type Electro-Magnetic Currentmeters (ECM) with 8-Hz sampling frequency were used. The sensors were installed on circular masts, three at each cross-shore location. Due to intrinsic limitations, the ECMs could not be placed nearer than 15 cm from the bottom. Thus, the ECMs measurements covered the vertical range between the mean surface elevation and 15 cm above the bottom, every 5 cm apart. Two Acoustic Doppler Velocimeters (ADVLab) were used to measure the three-component flow velocities across the

Table 1
Characteristics of the considered wave conditions

Wave condition	Symbol	H, H_{rms} (m)	T_p (s)	H_{rms}/L	No. Ursell, $U_r = \frac{16}{3} K^2 \kappa^2$	x_b (m)	H_b (m)	d_b (m)	Breaking type
A (reg.)	○	0.21	2.50	0.024	1.876	40.5	0.30	0.41	Spilling
B (reg.)	+	0.21	3.50	0.015	4.728	42.0	0.35	0.45	Plunging
C (reg.)	×	0.38	3.50	0.027	8.556	46.5	0.58	0.56	Plunging
D (irreg.)	△	0.21	2.50	0.024	1.876	—	—	—	—

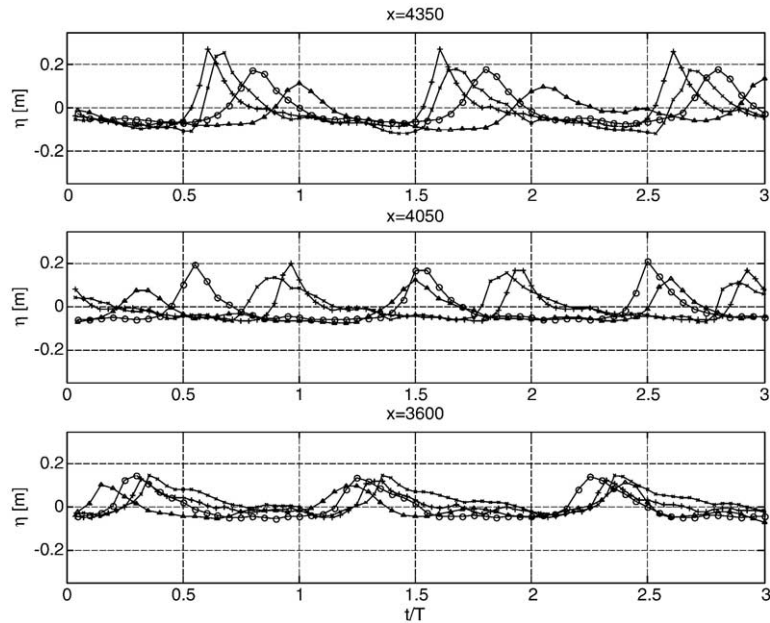


Fig. 3. Behavior in the dimensionless time, t/T , of the free-surface elevation η at three selected measurement transects: wave A (\circ), wave B ($+$), wave C (\times), and wave D (Δ).

bar at both 25- and 50-Hz sampling frequencies. The sensor cases were fixed to a supporting frame which allowed exact adjustments of the vertical position. The two ADV Labs measured velocities at each transect along the bar with a vertical spacing ranging between 5 and 7 cm for 45 points. The description of the ADVP functioning (Takeda, 1991) and set-up is given in the following.

3. Water surface elevation

The cross-shore variation of the water surface elevation has been assessed by visual observations and by means of data analysis. For the adopted incident wave characteristics, two different surf zones were visually detected. Waves shoaled until the first breaking point (at $x \approx 4000$ cm), then broke and decayed, reforming and shoaling again (at $x < 3200$ cm), where a second breaking occurred, nearer the shoreline ($x < 2200$ cm). All waves reformed around $x \approx 3200$ cm, which limited the length of the first surf zone. Across the bar, the behavior in dimensionless time, t/T , of the free-surface elevation, η , at three selected transects is shown in Fig. 3 where $t/T=0$ corresponds to the external event triggering the acquisitions by all the instruments, including all the velocimeters. Inspection of

Fig. 3 reveals that values of H_{rms} decrease landward and reach almost the same value at $x=3600$ cm, with most of reduction occurring between the first two of the transects ($x=4350$ and 4050). For all tests, Fig. 4 exhibits the cross-shore variation of the normalized wave height (H_{rms}/d) as a function of the dimensionless breaking position (x/x_b). All wave conditions present a similar behavior. Because of the different type of breaking, maximum values of H_{rms}/d at the breaking point for waves B and C are slightly larger than for the case of wave A.

4. ADVP functioning and set-up

Functioning of the ADVP is based on the Doppler effect. Acoustic waves with frequency, f_e , and speed, c , are emitted by a sensor and pass through space filled with targets moving with a velocity having a radial component, V , in the direction of the ultrasonic beam. The beams from the transducer are reflected by the targets. The back scattering wave has the frequency f_s . The following relationship can be given:

$$cf_D = \gamma V f_e \quad (1)$$

where $f_D = f_e - f_s$ is the Doppler shift frequency and $\gamma = 2$ since the moving target represents both a receiver and an emitter. The

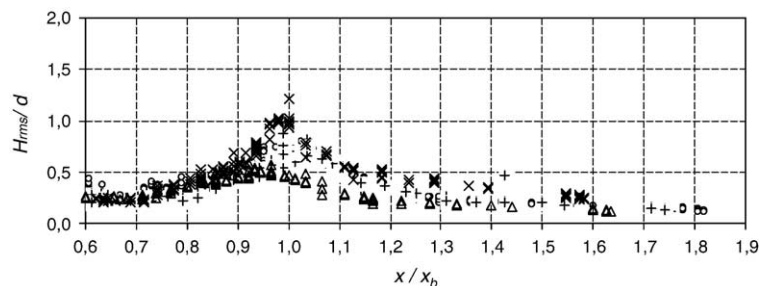


Fig. 4. Cross-shore variation of H_{rms}/d for the four adopted wave conditions.

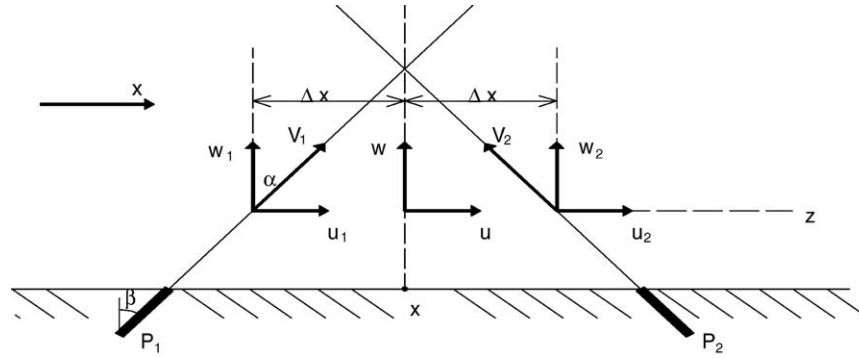


Fig. 5. The two ADVP probes, the coordinate system, and the symbols' description.

knowledge of c , f_c , and f_s allows the calculation of V . It's well known that the quality of the acoustic measurement is highly influenced by the concentration and size of bubbles. With regard to the influence of concentration, Longo (submitted for publication) reports the following relationship between the air and water celerity

$$\frac{c_w^2}{c_a^2} = \left(1 - v + \frac{vK_a}{K_w}\right) \left(1 - v + \frac{v\rho_a}{\rho_w}\right) \quad (1a)$$

which does not apply to high frequency propagation (Medwin and Klein, 1998) and where c_w =celerity in pure water, c_a =celerity in air, K_w =water compressibility, K_a =air compressibility, ρ_w =water density, ρ_a =air density and v =bubble volume fraction. Eq. (1a) shows that the reliability of the acoustic measurements depends on the air bubble concentration and certainly on the considered transect in a surf zone.

Some researchers (Graf, 1996; Lemmin and Rolland, 1997), for uniform flow conditions, showed that two ultrasonic probes installed symmetrically with respect to the vertical allow the correct observation of the flow field at a given transect x (Fig. 5). The present experimental investigation has been established in collaboration with the probe designer and has considered a similar scheme with two ultrasonic probes having a 1-MHz emitting frequency and a near field of 2.4 cm where the velocity can not be measured accurately. The angle between the probe's ultrasonic beam axis and the vertical, β , was equal to 30° . The probes were fixed in PVC supports spaced 10 cm apart, located in a 14-cm wide longitudinal trench below the bottom and running along the beach profile. The near field fell into the PVC support. The use of a PVC support was considered because, as specified by the manufacturer, the

probes could not be reliable any more after a permanence of several hours in the water.

In order to maintain the continuity of the bottom and to avoid any disturbance of the wave field, where the sensors were not in place, the trench was covered with thin PVC plates. The geometrical angle β does not correspond to the one used in the data analysis due to the refraction of the ultrasonic beam as it propagates through the PVC support to the water, with different sound speeds. Neglecting the effect of bubbles and assuming a constant sound speed in water of 1470 m/s, the refracted angle, α , has been found $\approx 24^\circ$; the effect of the moderate angle of the bottom slope at the bar ($< 1^\circ$) has been neglected. The two probes' ultrasonic beams intersected at $z_b = 10.79$ cm where $\Delta x \approx 0$, with z_b representing the elevation with respect to the bottom positive upward and zero at the bottom. This set-up allowed to obtain near-simultaneous velocity profile measurements over the water column at points spaced about 2.2 mm apart, and undisturbed from any intrusive equipment. The ADVP sampling frequencies ranged from 13.4 to 21.1 Hz, depending on the setting and calibration of the instrument for a certain run (Table 2). The trigger signal synchronised the acquisitions made with the ADVP with those from all the other instruments.

5. Velocity data pre-processing

5.1. ADVP

Previous studies verified the ADVP efficiency for the uniform flow case (Graf, 1996; Lemmin and Rolland, 1997) and for the case of unsteady flow in an open channel with a rough bed (Song and Graf, 1996). In those studies, the horizontal, u , and vertical, w , velocity components were

Table 2
Example of the ADVP set-up characteristics

Wave condition	A	A	B	B	C	C	D
x [cm]	4050	3600	4150	3600	4350	3600	3600
Water depth [cm]	39.3	45.0	40.0	45.0	45.0	45.0	45.0
US beam length [cm]	35.5	39.0	34.2	39.0	35.5	39.0	39.0
Sampling frequency [Hz]	13.4	21.1	13.8	13.4	13.4	15.5	13.4
Pulse repetition frequency [Hz]	2016	1838	2083	1344	2016	1344	1344
Burst length [cycles]	8	8	8	8	8	8	8

determined under the assumption that the flow is uniform with the relationships

$$u = \frac{V_1 - V_2}{2\sin\alpha} \quad \text{and} \quad w = \frac{V_1 + V_2}{2\cos\alpha} \quad (2)$$

on the basis of the velocity components V_1 and V_2 measured along the ADVLab beam axis. In fact, it has been assumed that the values of u and w are identical at the same elevation but at different horizontal location. This assumption is valid only for steady uniform flow; when considering an oscillatory flow, in general, $u_1 \neq u_2$ and $w_1 \neq w_2$. With the hypothesis that $\Delta x \ll L$, the following Taylor's expansions can be written (N. Kobayashi and G.R. Tomasicchio, personal communication, June 26, 2001)

$$u_1(x - \Delta x) \approx u(x) - \Delta x \frac{\partial u}{\partial x} \quad \text{and} \quad w_1(x - \Delta x) \approx w(x) - \Delta x \frac{\partial w}{\partial x} \quad (3a)$$

$$u_2(x + \Delta x) \approx u(x) + \Delta x \frac{\partial u}{\partial x} \quad \text{and} \quad w_2(x + \Delta x) \approx w(x) + \Delta x \frac{\partial w}{\partial x} \quad (3b)$$

Radial velocities V_1 and V_2 can be expressed as

$$V_1 = u_1 \sin\alpha + w_1 \cos\alpha \quad \text{and} \quad V_2 = -u_2 \sin\alpha + w_2 \cos\alpha \quad (4)$$

Combining Eqs. (2) and (3a), (b), it results

$$u = \frac{V_1 - V_2}{2\sin\alpha} + \frac{\Delta x \partial w / \partial x}{\tan\alpha} \quad \text{and} \quad w = \frac{V_1 + V_2}{2\cos\alpha} + \Delta x \frac{\partial u}{\partial x} \tan\alpha \quad (5)$$

Present experimental data have not allowed determination of the correction term $\partial u / \partial x$; therefore, u has been determined solely with Eq. (2). Use of Eq. (2) can be extended to the oscillatory flow case when $\Delta x = 0$ or if

$$(V_1 - V_2) \gg \Delta x \frac{\partial w}{\partial x} \quad \text{and} \quad (V_1 + V_2) \gg \Delta x \frac{\partial u}{\partial x} \quad (6)$$

It is worth noting that investigators are likely to go the trouble of using high frequency, high resolution Doppler Velocity Profilers to make instantaneous measurements of flow around and beneath breaking to study small-scale features such as turbulence and vortex generation. In this case, the spatial gradients in the velocity field can only be neglected for flow fluctuations with small wave numbers. There is certainly some critical wave number allowing to neglect the spatial gradients in the velocity field. Unfortunately, the present research does not allow any big conclusion on this important subject because of an adopted too small range of variation of the wave number.

In the following, for conditions adopted here, the validity of Eq. (2) to determine the horizontal velocity distributions induced by an oscillatory flow in the surf zone is discussed.

5.2. ECM and ADVLab

All temporal velocity series sampled by the ECMs and ADVLabs have been initially screened for erroneous readings: it has been admitted that two consecutive readings are affected

by “noise” whenever the corresponding acceleration is larger than two times the acceleration of gravity, g ; accelerations larger than $2g$ are admitted as unphysical. The level of the signal-to-noise (SNR) ratio and of the auto-correlation function of all velocity components from the ADVLab has been determined. Signals with SNR less than 20 dB and auto-correlation values less than 90% have been disregarded avoiding any uncertainty on noise influence (Goring and Nikora, 2002). Table 3 reports the number of disregarded data files.

Systematic comparison of the screened data has showed that most of the measured velocity time series have an agreement similar to that presented in Fig. 6. This figure shows time series of the horizontal velocity component, u , obtained by one ADVLab, one ECM, and the ADVP at approximately the same vertical and horizontal position, although at different repetitions of the same wave condition. Therefore, differences in the time series reflect a different measuring error, a non-synchronous reading, and a slightly different positioning.

6. Acoustic Doppler data comparison

A time series comparison of data from the two different acoustic Doppler instruments would require simultaneous measurements at the same elevation within a given transect. Since the experiments aimed at covering three different wave conditions at several instrument's locations, there was no logistical opportunity to systematically repeat such measurements with the two instruments. The comparisons have been performed only at transect $x = 3600$ cm in the inner region at $z_b = 10.50$ cm where $\Delta x \approx 0$. Consequently, the temporal series comparison of u from the ADVP and the ADVLab has been conducted only for this case for each of the four wave conditions. For the remaining cases in the outer region of the surf zone, the estimate of the ADVP reliability has been based on the comparison of the measured vertical distributions of the time-mean horizontal velocities.

6.1. Wave breaking region

The horizontal velocity profiles at selected instants in one period after the trigger signal ($t/T = 0$) are shown in Figs. 7 and 8 and are representative of all cases. The vertical axis is the ratio of z_b to the local water depth, d ; the horizontal axis represents u , where positive values refer to velocities along the wave propagation direction. In particular, the velocity profiles for wave conditions A and C at $x = 4050$ and 4350 cm ($x/x_b = 1.00$ and 0.935 , and $H_{rms}/L = 0.054$ and 0.043 , respectively) are shown; their shape discontinuities and the large

Table 3
Number of ADVLab disregarded acquisitions

Wave condition	No. of repetitions	Disregarded acquisitions
A (reg.)	52	6
B (reg.)	47	4
C (reg.)	49	14
D (irreg.)	49	6

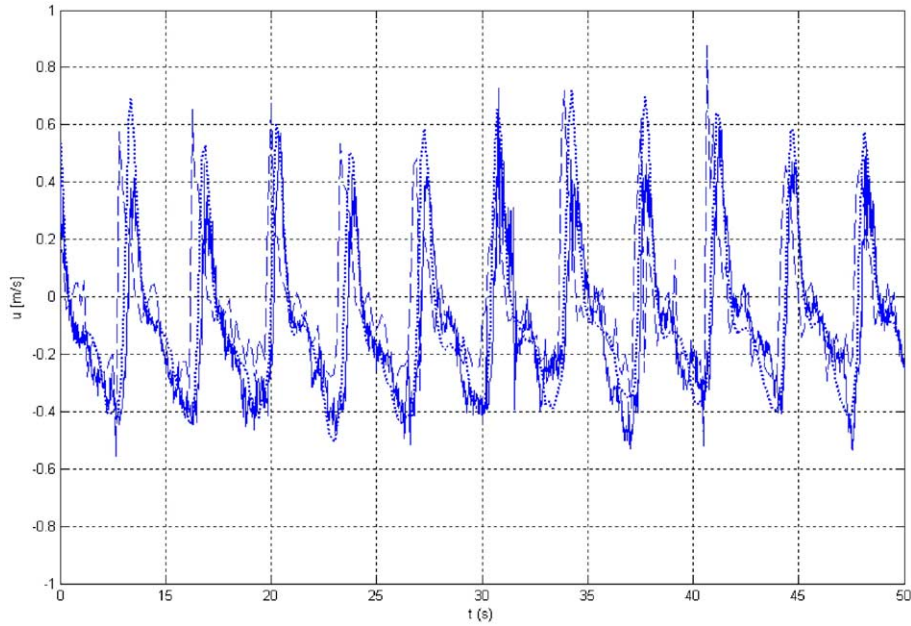


Fig. 6. Wave B, $x=4050$ cm; $z_b \approx 15$ cm; behavior in time of the horizontal velocity component as measured by the ADVLab (solid), the ADVP (dashed) and the ECM (dotted).

spreading make evident that the ADVP measurement results are invalid. Reference to the synchronous temporal series of the water surface elevation (Fig. 3) points out that errors increase at the passage of the wave crest. Errors and sudden sign reversal are probably due to the fact that the acoustic profiler does not take into account the variation of the sound speed due to the inclusion of bubbles in the water in which the concentration certainly increases at the passage of the crest. Profiles in Fig.

8 seem sufficiently reliable, but before accepting them, a comparison with measurements from the ADVLab and the ECMs is necessary.

Time averaging for a minimum record length of 50 waves has been considered for calculating the horizontal time-mean flow from screened measurements with the three different velocity meters. In Fig. 9 undertow values for wave condition C at $x=4350$ cm are shown. The vertical axis is z_b/d ; the

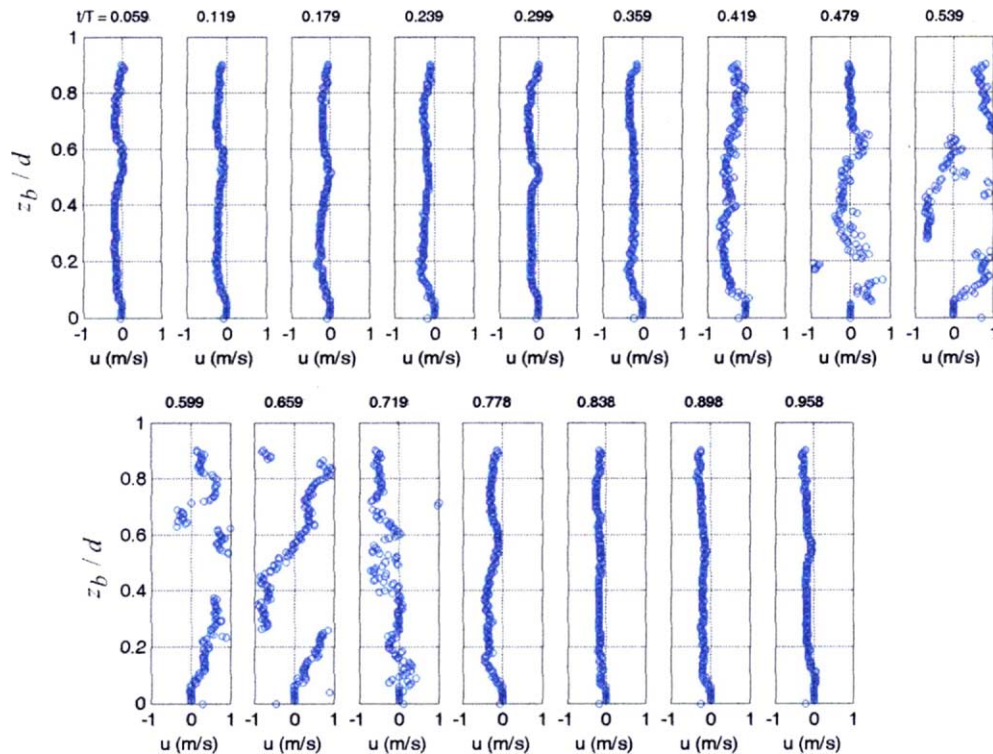


Fig. 7. Horizontal velocity profiles: wave condition A, $x=4050$ cm, $x/x_b=1$.

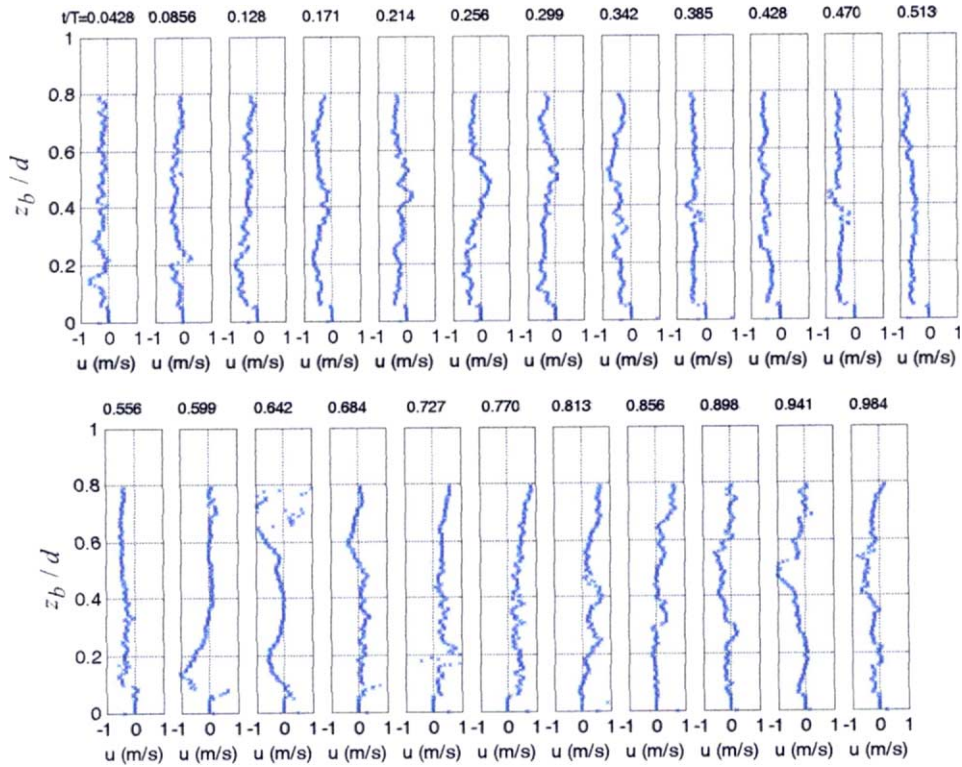


Fig. 8. Horizontal velocity profiles: wave condition C, $x=4350$ cm, $x/x_b=0.935$.

horizontal axis is the undertow value, U . Still water level is indicated in the figure by zero. The solid line represents the vertical distribution of U from the ADVP. Undertow data from the ADVLab (\bullet) and ECM ($*$) sensors are in satisfactory agreement with each other, although they refer to different wave attacks and cross-flume lines. The ADVP undertow profiles appear to be largely influenced by clouds of bubbles and foam causing an underestimation in undertow. In general, it has been observed that the underestimation substantially increases near the incipient breaker location (when x/x_b approximates 1).

6.2. Bore-like region

Figs. 10 and 11, typical of all cases, show selected velocity profiles one period after the trigger signal for wave conditions D and C, respectively, at $x=3600$ cm in the inner region of the surf zone ($x/x_b=0.774$ for wave condition C, and $H_{rms}/L=0.024$ and 0.027 , for D and C, respectively). The simultaneous measurements from the ADVLab placed at $z_b=10.5$ cm are also shown. The agreement can be considered satisfactory at all phases when considering that the two

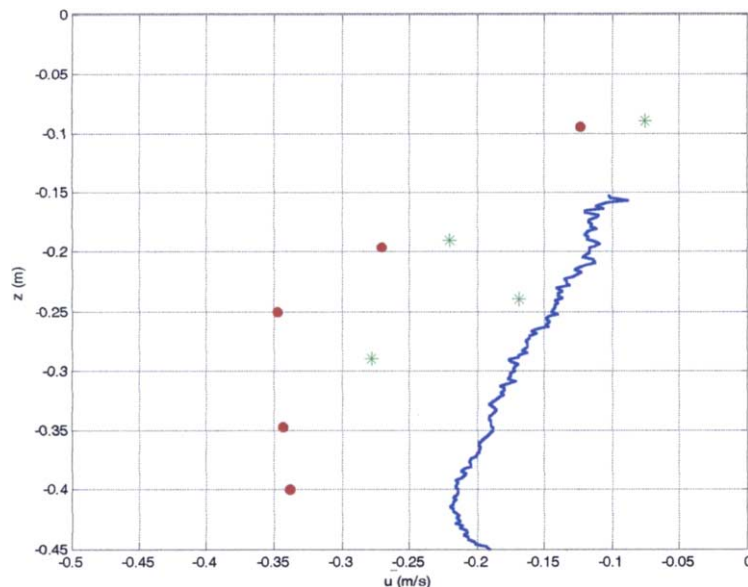


Fig. 9. Wave C, $x=4350$ cm, $x/x_b=0.935$: comparison of ADVP (solid line), ADVLab (\bullet) and ECM ($*$) undertow data.

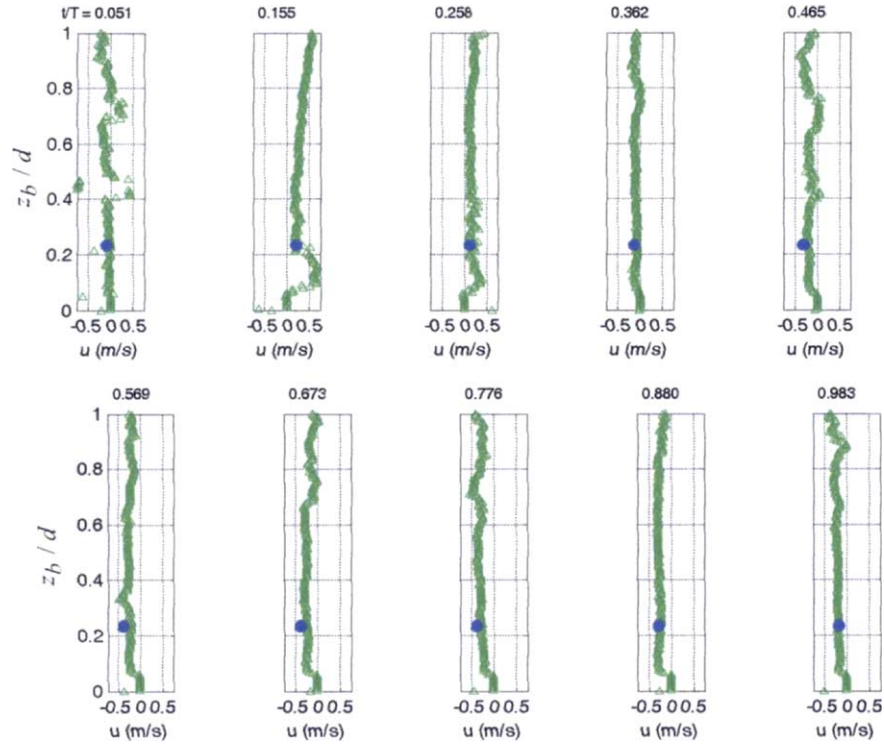


Fig. 10. Horizontal velocity profiles: wave condition D, $x=3600$ cm; comparison of ADVP (Δ) and ADVLab (\bullet) simultaneous data at $z_b=10.5$ cm.

instruments were not positioned at the same cross-flume line. Inspection of (Figs. 10, 11 and 3) reveals that the agreement is slightly poorer when the wave crest passes.

In order to estimate the effect of extending the use of Eq. (2) for the horizontal velocity component to oscillatory flow, in analogy to the outer region case, the undertow profiles from

the three different velocimeters have also been considered at the inner region where the effects of wave breaking are less intense. Fig. 12 exhibits a certain agreement of mean horizontal velocity data from the three measuring devices. As a first impression the use of Eq. (2) for u may be accepted for most of the oscillatory flow conditions analysed here, and

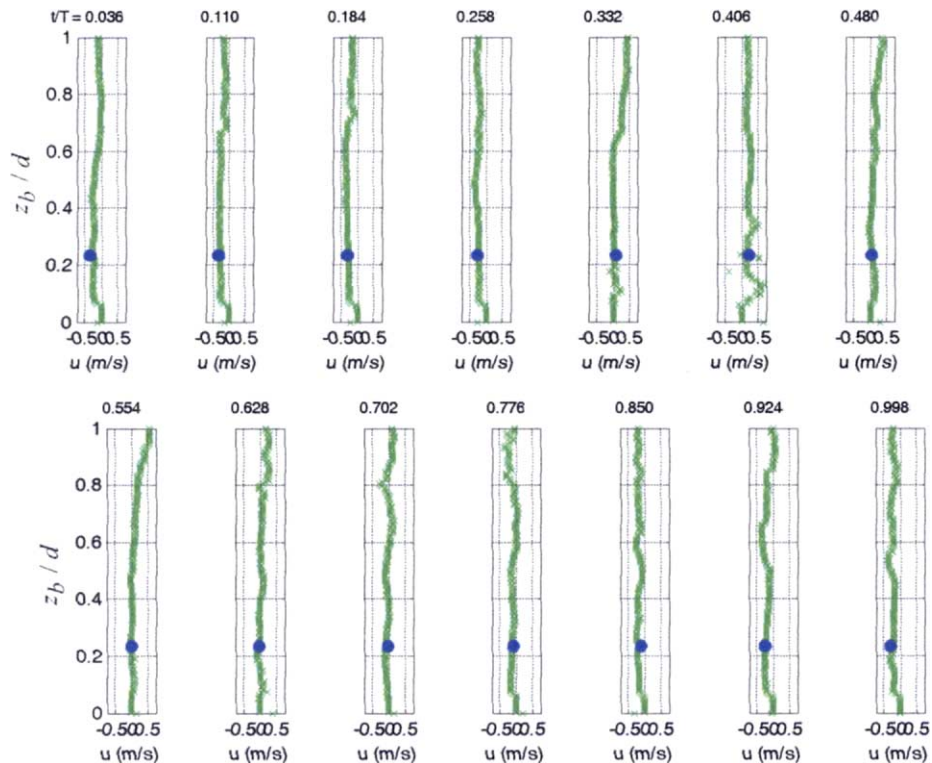


Fig. 11. Horizontal velocity profiles: wave condition C, $x=3600$ cm, $x/x_b=0.774$; comparison of ADVP (\times) and ADVLab (\bullet) simultaneous data at $z_b=10.5$ cm.

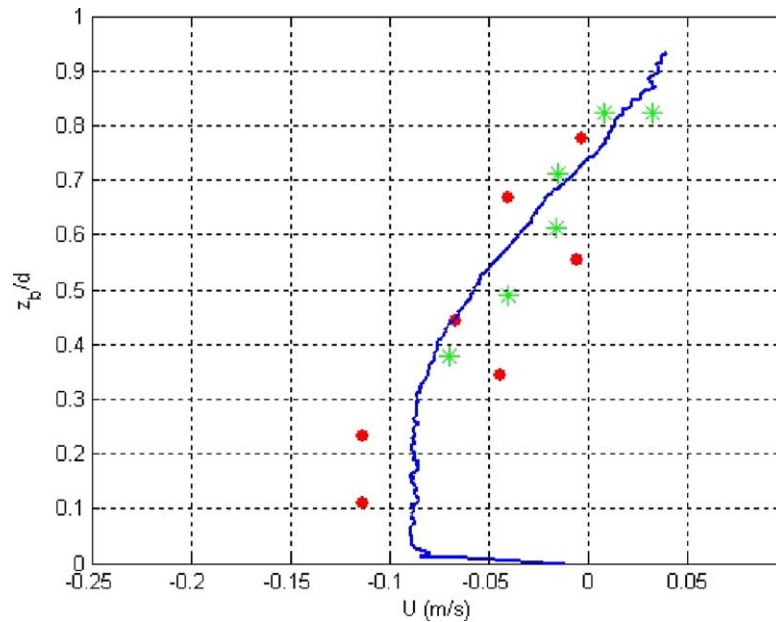


Fig. 12. Wave C, $x=3600$ cm, $x/x_b=0.774$: comparison of ADVP (solid line), ADVLab (\bullet) and ECM ($*$) undertow data.

thus, the limitation from considering $\partial u/\partial x$ negligible may be certainly minor with respect to the measuring errors determined by the presence of clouds of bubbles along the entire water column.

7. Discussion

The present contribution aims to perform a verification of the reliability of an ADVP in measuring the flow field induced by regular and irregular breaking waves on a sloping beach. In the flow field conditions adopted in the present experimental activity, the instrument had an acceptable performance at transects in the inner region of the surf zone with values of $H_{rms}/L < 0.04$ and having $x/x_b < 0.8$ where $H_{rms}/d < 0.5$ (Fig. 4). At the rest of the transects in the outer region, the system was highly influenced by air inclusion in the breaking wave that affects the sound speed significantly. In this case, the shape of the observed velocity profiles indicates that the use of the ADVP is limited because bubbles are generated and transported as waves break at shallow water (Thorpe, 1982).

8. Conclusions

An experience has been gained with the use of an ADVP at wave breaking in large-scale lab measurements. Measured horizontal velocity components from the ADVP have been analysed and discussed for breaking waves, as well as in the inner surf zone. As expected, at the outer region of the surf zone, in comparison to the ADVLab and ECM, the ADVP appears less reliable, perhaps because the measured Doppler shift is affected by the various effects along the entire path of the sound, unlike for point measurements. At the transects where the effects of wave breaking are less intense and near wave reforming, the ADVP horizontal velocity is in

reasonable agreement with the rest of the measurements. In particular, differences in the performance of the ADVP in the incipient breaking region compared to the bore-like region indicate that, although the ADVP appears much noisier than the ADVLabs and the ECMs, the role of bubbles at outer zone is prevalent in its measuring error and may give a large underestimation (even of about 50%) of the mean horizontal velocity component with respect to the single point instruments.

Furthermore, the agreement of measurements in the bore-like region where the role of air inclusion is minor indicates that, for the characteristics of the considered barred beach and for the adopted wave conditions, the extension of Eq. (2) for the horizontal velocity component to the oscillatory flow case generates a negligible error for estimating mean flow (undertow).

Acknowledgments

The writer gratefully acknowledges Prof. N. Kobayashi from University of Delaware for the fruitful and stimulating discussions and Dr. F. Sancho from LNEC, Lisbon, for coordinating the SPANWAVE project funded by the European Commission, Training and Mobility of Researchers Programme—Access to Large-scale Facilities, under contract no. ERBFMGECT9500073.

The author also thanks the two anonymous reviewers that provided many constructive comments that have been incorporated into the manuscript.

References

- Cox, D.T., Kobayashi, N., 2000. Identification of intense, intermittent coherent motions under shoaling and breaking waves. *J. Geophys. Res.* 105 (C6), 14223–14236.

- Cox, D.T., Kobayashi, N., Okayasu, A., 1994. Vertical variations of fluid velocities and shear stress in surf zones. *Proc. 24th Int. Conf. Coastal Engng.*, vol. 1. ASCE, Kobe, pp. 99–112.
- Cox, D.T., Kobayashi, N., Okayasu, A., 1995. Experimental and numerical modeling of surf zone hydrodynamics. Res. Report No. CACR-95-07. Univ. of Delaware.
- Deane, G.B., 1997. Sound generation and air entrainment by breaking waves in the surf zone. *J. Acoust. Soc. Am.* 102 (5), 2671–2689.
- Dean, R.G., Dalrymple, R.A., 1984. *Water Wave Mechanics for Engineers and Scientists*. World Scientific, Singapore.
- Deane, G.B., Stokes, M.D., 1999. Air entrainment processes and bubble size distributions in the surf zone. *J. Phys. Oceanogr.* 29, 1403–1993.
- Deane, G.B., Stokes, M.D., 2002. Scale dependence of bubble creation mechanisms in breaking waves. *Nature* 418 (22), 839–844. August.
- Doering, J.C., Donelan, M.A., 1997. Acoustic measurements of the velocity field beneath shoaling and breaking waves. *Coast. Eng.* 32, 321–330.
- Eckert, S., Gerbeth, G., 2002. Velocity measurements in liquid sodium by means of ultrasound Doppler velocimetry. *Exp. Fluids* 32, 542–546.
- Farmer, D.M., Deane, G.B., Vagle, S., 2001. The influence of bubble clouds on acoustic propagation in the surf zone. *IEEE J. Oceanic Eng.* 26, 113–124.
- Goring, D.G., Nikora, V.I., 2002. Despiking Acoustic Doppler Velocimeter data. *J. Hydraul. Eng.* 128 (1), 117–126.
- Graf, W.H., 1996. Bed-load transport in unsteady open-channel flow. Opening Conference at the XXV Italian Congress of Hydraulics, Torino, Italy.
- Kennedy, A.B., Chen, Q., Kirby, J.T., Dalrymple, R.A., 1999. Boussinesq modeling of wave transformation, breaking and runup: I. One dimension. *J. Waterw., Port, Coast., Ocean Eng.* 126 (1), 39–47.
- Kraus, N.C., Smith, J.M., 1994. SUPERTANK laboratory data collection project. Tech. Rep. CERC-94-3, US Army Corps of Engineers, Waterways Experiment Station.
- Lemmin, U., Rolland, T., 1997. Acoustic velocity profiler for laboratory and field studies. *J. Hydraulics Engng.*, vol. 125. ASCE, pp. 1089–1098.
- Leighton, T.G., Phelps, A.D., Ramble, D.G., 1996. Acoustic bubble sizing: from the laboratories to surf zone trials. *Acoust. Bull.* May/June, 5–13.
- Longo, S., Losada, I.J., Petti, M., Pasotti, N., Lara, J.L., 2001. Measurements of breaking waves and bores through a USD velocity profiler, Tech. Report UPR/Uca_01_2001, Universidad de Cantabria.
- Longo, S., submitted for publication. Air bubble effects on UltraSound velocity measurements. *Experiments in Fluids*.
- Medwin, H., Klein, C.S., 1998. *Fundamentals of Acoustical Oceanography*. Acad. Press.
- Nadaoka, K., Kondoh, T., 1982. Laboratory measurements of velocity field structure in the surf zone by LDV. *Coast. Eng. Jpn.* 25, 125–145.
- Nielsen, K.D., Weber, L.J., Muste, M., 1999. Capabilities and limits for ADV measurements in bubbly flows. XXVIII IAHR Congress, Graz, pp. 382–392.
- Okayasu, A., 1989. Characteristics of turbulence structure and undertow in the surf zone, Ph. D. dissertation, University of Tokyo.
- Sanchez-Arcilla, A., Roelvink, J.A., O'Connor, B.A., Reniers, A., Jimenez, J.A., 1995. The Delta Flume '93 experiment. *Proc. Coastal Dynamics '95*, Gdansk, pp. 488–502.
- Sancho, F.E., 1999. Equilibrium barred-beach profile. 1st Portuguese Conference on Harbour and Coastal Engng., Porto (in Portuguese).
- Sancho, F.E., Mendes, P.A., Carmo, J.A., Neves, M.G., Tomasicchio, G.R., Archetti, R., Damiani, L., Mossa, M., Rinaldi, A., Gironella, X., Arcilla, A.S., 2001. Wave hydrodynamics over a barred beach. *Proc. Waves 2001*. ASCE, S. Francisco, pp. 1170–1179.
- Sarpkaya, T., Isaacson, M., 1981. *Mechanics of Wave Forces on Offshore Structures*. Van Nostrand Reinhold Company, New York.
- Song, T., Graf, W.H., 1996. Velocity and turbulence distribution in unsteady open-channel flows. *J. Hydraulic Engng.*, vol. 122. ASCE, pp. 141–154.
- Stive, M.J.F., 1980. Velocity and pressure field of spilling breakers. *Proc. 17th Int. Conf. Coastal Engng.*, vol. 1. ASCE, Sydney, pp. 547–566.
- Takeda, Y., 1991. Ultrasonic Doppler method or velocity profile measurement in fluid dynamics and fluid engineering. *Exp. Fluids* 26, 177–178.
- Thorpe, S.A., 1982. On the clouds of bubbles formed by breaking wind-waves in deep water, and their role in air–sea gas transfer. *Philos. Trans. R. Soc. Lond.* A304, 155–210.
- Ting, F.C.K., Kirby, J.T., 1994. Observation of undertow and turbulence in a laboratory surf zone. *Coast. Eng.* 24, 51–80.
- Tomasicchio, G.R., Neves, G.M., Sancho, F., 2001. Wave reflection analysis at a barred beach. *Proc. Coastal Dynamics '01*, vol. 1. ASCE, Lund, pp. 146–156.
- USACE, 1998. *Coastal Engineering Manual*, Waterways Experiment Station. U.S. Government Printing Office, Washington, D.C.